

Microgravity Reduces the Differentiation and Regenerative Potential of Embryonic Stem Cells

Elizabeth A. Blaber,^{1,2} Hayley Finkelstein,¹ Natalya Dvorochkin,¹ Kevin Y. Sato,³
Rukhsana Yousuf,¹ Brendan P. Burns,^{2,4} Ruth K. Globus,¹ and Eduardo A.C. Almeida¹

Mechanical unloading in microgravity is thought to induce tissue degeneration by various mechanisms, including inhibition of regenerative stem cell differentiation. To address this hypothesis, we investigated the effects of microgravity on early lineage commitment of mouse embryonic stem cells (mESCs) using the embryoid body (EB) model of tissue differentiation. We found that exposure to microgravity for 15 days inhibits mESC differentiation and expression of terminal germ layer lineage markers in EBs. Additionally, microgravity-unloaded EBs retained stem cell self-renewal markers, suggesting that mechanical loading at Earth's gravity is required for normal differentiation of mESCs. Finally, cells recovered from microgravity-unloaded EBs and then cultured at Earth's gravity showed greater stemness, differentiating more readily into contractile cardiomyocyte colonies. These results indicate that mechanical unloading of stem cells in microgravity inhibits their differentiation and preserves stemness, possibly providing a cellular mechanistic basis for the inhibition of tissue regeneration in space and in disuse conditions on earth.

Introduction

ON EARTH, ORGANISMS ARE constantly subjected to gravity-generated forces [1] that provide an array of mechanical stimulation essential for normal cell and tissue function. The influence of gravity-generated forces on the human body is especially evident in the effects of physical exercise on the skeleton. Specifically, mechanical loading of tissues promotes tissue regenerative health via stimulation of adult stem cell proliferation and differentiation. On the other hand, mechanical unloading experienced during spaceflight-induced microgravity (μ g) conditions, and other disuse conditions including prolonged bedrest, induce degenerative changes in physiology, including tissue regenerative deficits and tissue loss, such as observed in bone and muscle. Because of this, it is important to understand mechanical unloading-mediated changes in stem cells that may result in altered tissue regenerative health.

Stem cells derived from all three germ layers are known to be affected by μ g, including cells originating from the ectoderm lineage with a decreased capacity to differentiate into immune cells [2], cells from the mesoderm lineage (hematopoietic stem cells) with a diminished capacity to differentiate into blood tissue [3], and endoderm-derived tissues such as the lungs and pancreas [4]. The rate of stem cell-based

regeneration, however, is tissue-specific and highly variable—ranging from renewal of intestinal epithelial cells every 2 or 3 days, to about 120 days for red blood cells, to very slow renewal rates of years in cells such as cardiomyocytes [5,6]. Because of the widely variable tissue-specific regenerative renewal times, μ g is likely to affect regeneration at different rates, with different physiological outcomes.

While several studies have investigated the role of increased mechanical load in promoting cell proliferation and differentiation [7–9], few have investigated the effects of removing that load in μ g. Some studies using “simulated microgravity” (SMG) have investigated its impact on embryonic stem cell (ESC) properties, including cell numbers, adhesion capabilities and apoptosis rates [10], and differentiation into periodontal ligament cells [11], and liver stem cells [12]. However, while SMG-generating devices, such as the rotating wall vessel (RWV) and random positioning machine (RPM), may randomize the gravity vector, they do not reduce the overall mechanical stimulation from fluid flow shear and hydrostatic pressure that adherent cells experience in these vessels, thus limiting the value and accuracy of the models.

Previously, we have described mechanical unloading-associated stem cell regenerative alterations in bone from mice exposed to μ g [13,14] and are now studying mechanistic

¹Space Biosciences Division, NASA Ames Research Center, Moffett Field, California.

²School of Biotechnology and Biomolecular Sciences, University of New South Wales, Sydney, Australia.

³FILMSS Wyle, Space Biology, NASA Ames Research Center, Moffett Field, California.

⁴Australian Centre for Astrobiology, University of New South Wales, Sydney, Australia.

aspects of these findings using a model of early lineage commitment during mouse embryonic stem cell (mESC) early differentiation into embryoid bodies (EBs). When mESCs are maintained on a gelatin matrix with the pluripotency factor leukemia inhibitory factor (LIF), or in the presence of an embryonic fibroblast feeder layer, these cells remain pluripotent. However, when the cells are removed from contact with the feeder layer, or when LIF is removed from the culture medium in combination with growing the mESCs on ultra-low adhesion substrates, mESCs form three-dimensional spherical cell aggregates, known as EBs, and begin to spontaneously differentiate [15,16].

As EB differentiation continues, the cells follow a reproducible temporal pattern that recapitulates early embryogenesis although without organized patterning of tissues and organs [15,16]. Over time, EBs increase in cell number and complexity as cells form structures comparable to embryonic germ layers including a wide variety of cell types, such as, cardiomyocytes, hematopoietic cells, and neurons [17–19]. Although EB formation specifically models stem cell differentiation into embryonic tissues, this process has significant similarities with adult stem cell-based tissue regeneration [20], thus EBs have a broad utility to investigate the effects of mechanical unloading on adult tissue regenerative processes, too.

Here, we report results from using the EB stem cell differentiation model to study mESC early lineage commitment in μg in the NASA Space Tissue Loss (STL) experiment performed on the Space Shuttle Discovery during the NASA STS-131 mission. Our broad hypothesis underlying this experiment is that mechanical unloading of cells and tissues in μg alters the proliferation and differentiation patterns of stem cells resulting in decreased stem cell-based tissue regenerative potential in space. In this study, we found that spaceflight in μg promoted the maintenance of EB stem cell gene expression and post- μg reloading differentiation potential, defined as “stemness”, and inhibited the appearance of differentiation markers for multiple tissue lineages. These findings may have important implications for the maintenance of tissue regenerative health in both astronauts during short and long-duration spaceflight in μg conditions, and for humans on earth.

Experimental Procedures

mESC culture

mESCs were cultured on 10 cm tissue culture treated dishes coated with 0.1% gelatin. Cells were cultured in mESC medium (DMEM supplemented with 15% FBS, 4 mM L-glutamine, 1 \times nonessential amino acids, 1 mM sodium pyruvate, 1% antibiotic solution (penicillin/streptomycin), trace β -mercaptoethanol, and 10 ng/mL LIF. The medium was changed daily and cells were passaged every 48 h using 0.25% trypsin solution.

mESC differentiation–formation of embryoid bodies

Before differentiation 5.0×10^6 mESCs were removed and fixed in RNAlater II to serve as a baseline control for gene expression analysis. To form EBs, 59 h before spaceflight LIF was removed from the mESC culture media and cells were passaged using 0.25% trypsin solution and

transferred to ultra low adhesion 10 cm tissue culture dishes, thereby preventing reattachment of cells. A seeding density of 5.8×10^6 mESC per dish was used. Half of the medium was changed after 24 h to prevent loss of cell density.

Spaceflight

Cell culture module. The STL experiment was conducted within the Cell Culture Module (CCM; Tissue Genesis, Inc.) hardware in a middeck locker on the space shuttle. The CCM is a fully automated system and provides gas perfusion, medium recirculation, and medium routing by peristaltic pumps and pinch valves, reagent injection (RNAlater II), and sample collection. Cells were cultured within hollow fiber bioreactors (Spectrum Labs), which allowed full submersion of the cells in the extra-capillary space (ECS) with 60 mL of medium recirculating through the intracapillary space. Medium nutrients diffused through the hollow fibers protecting cells from fluid flow shear forces that would otherwise negate the low mechanical loading of the μg environment. Bioreactors were primed with isopropanol for 10 min, washed with sterile water and stored in phosphate buffered saline (PBS). Bioreactors were also coated with 0.2% bovine serum albumin in PBS for 3 h at 37°C to prevent cell attachment. CCM flow paths were primed and operated with cell culture medium for 24–48 h. Fresh medium was replaced immediately before EB loading. Materials used in the fluid flow path included platinum-cured silicone tubing for CO₂ supply, pharmed tubing, and Hyclone medium bags.

STS-131 STL. At 24 h before launch, EBs were transferred from ultra low adhesion plates to 24 bioreactors plus spares, with one plate being loaded into each bioreactor. Bioreactors were integrated into the CCM for spaceflight ($n=12$), and into a separate CCM for synchronous ground controls ($n=12$). The spaceflight CCM was integrated into the space shuttle orbiter middeck locker 19 h before launch. The STL payload was flown during the STS-131 mission on the space shuttle Discovery (OV-103), which was launched on 5th April 2010 and landed on the 20th April 2010. The synchronous ground control unit was maintained at Kennedy Space Center under identical conditions to the spaceflight CCM except for exposure to μg . Four ground and four flight bioreactors were automatically fixed with 55 mL of RNAlater II 28 h before landing.

Postflight analysis of metabolic activity

Cell culture medium was collected 3 h postlanding from both the medium reservoirs and bioreactor ECS (1xg, $n=5$; μg , $n=8$). Glucose consumption and lactate production were measured using an i-STAT handheld blood analyzer using G and CG4+ cartridges.

Postflight embryoid body culture

Bioreactors were opened 3 h postlanding and equal volumes of EB suspensions were placed on 22 mm coverslips with either collagen or fibronectin and cultured for 9 days, or on 10 cm tissue culture treated dishes (1xg, $n=5$; μg , $n=8$). After 24 h, numbers of adherent EBs were quantified with light microscopy. Following 9 days of culture, colonies of contractile cells were identified and quantified with light microscopy. Cells were then washed with PBS and fixed in 4% paraformaldehyde on ice.

Embryoid body viability

To determine viability EBs were stained for 30 min with 0.5 μ M calcein and 1 μ M ethidium homodimer and imaged with fluorescence microscopy.

RNA isolation

EBs in RNAlater II were collected through a 40 μ m sieve and placed in TRIzol reagent for RNA isolation. Samples were then purified using an RNeasy Mini Kit with added Genomic DNA Elimination step (Qiagen) according to the manufacturer's protocol ($n=4$). RNA concentrations were measured using spectrophotometry (Nanodrop) and quality was determined by agarose gel electrophoresis.

Real time quantitative polymerase chain reaction analysis

To determine gene expression alterations in EBs differentiated in μ g compared to 1xg, Qiagen pathway-focused real time quantitative polymerase chain reaction (RT-qPCR) arrays were used. We specifically analyzed EBs exposed to spaceflight and fixed before Orbiter reentry (FLT) and EBs maintained on the ground at 1xg (GC) fixed at the same time as FLT samples and baseline mESCs that were preserved before EB formation. Arrays related to stem cells, the p53 pathway, and tissue lineage markers were examined and each pathway-focused array consisted of primer sets for 84 genes of interest, five reference genes (Gusb, Hprt1, Hsp90ab1, Gapdh, and Actb), one genomic DNA contamination control, three positive polymerase chain reaction

(PCR) controls, and three positive reverse transcription controls, on a 96-well plate.

For each sample, 0.1 microgram RNA was reverse transcribed into cDNA using RT² PreAMP cDNA Synthesis Kit (Qiagen) according to the manufacturer's protocol. The cDNA was then mixed with RT² SYBR Green/Rox qPCR master mix and 25 μ L was added to each well of the PCR plate. The plates were sealed with optical thin-walled 8 cap strips and RT-qPCR of sample arrays was performed using an Applied Biosystems 7500 Real Time PCR instrument. RT-qPCR conditions were as follows: one cycle 95°C for 10 min, 40 cycles of 95°C for 15 s and 60°C for 1 min, followed by one cycle of 95°C for 15 s, 60°C for 1 min, 95°C for 15 s, and 60°C for 15 s. Gene expression levels from all arrays were analyzed for alterations in expression levels as compared to controls ($n=4$, $P<0.05$) using a PCR Array Data Analysis Template (v3.2; SABiosciences). Data analysis was based on the $\Delta\Delta$ Ct method and gene expression levels were normalized to four reference genes (Gusb, Hprt1, Gapdh, and Actb).

Results

Post- μ g embryoid body viability and adhesion

EBs were either fixed on orbit with RNAlater II or returned live to earth following 15 days in μ g. EBs returned to earth live and corresponding 1xg controls were plated on either collagen (COL)- or fibronectin (FN)-coated 22 mm cover slips and 10 cm tissue cultures (TC) dishes within 4 h of the orbiter landing. Both μ g and 1xg EBs adhered similarly to COL and FN matrices or TC-treated plastic. Specifically, the number of

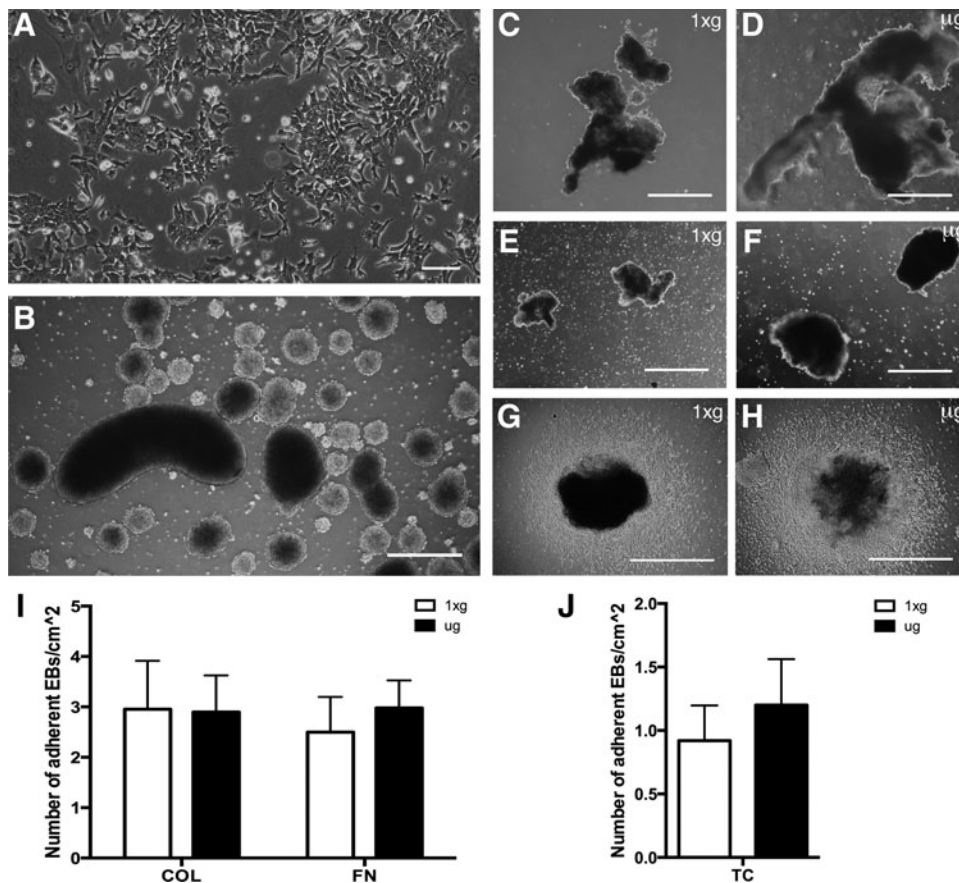


FIG. 1. Embryoid body (EB) formation and recovery post- μ g exposure. mESCs (A) were used to form EBs (B) for analysis of early lineage commitment and differentiation during and after 15 days spaceflight. EBs from 1xg bioreactor controls (C, E) and those recovered post- μ g exposure (D, F) showed similar appearance both in large sheets adherent to bioreactor fibers (C, D) and in smaller more EB-like cell clusters (E, F). No significant differences were found in the number of EBs that were recovered and adhered to collagen, COL, fibronectin, FN (I) and tissue culture-treated plastic, TC (J) matrices following differentiation in μ g (H) compared to 1xg; (G) conditions. Scale bar=100 μ m (A) or 500 μ m (B–H). 1xg, $n=5$; μ g $n=8$. 1xg, Earth's gravity; mESC, mouse embryonic stem cell; μ g, microgravity; TC, tissue cultures.

adherent EBs 150 μm in diameter or larger were counted, with no differences in adhesion observed (Fig. 1). Cell viability in adherent EBs and their outgrowth was determined with calcein AM and ethidium homodimer. No differences were found in the viability of EBs cultured in μg compared to those cultured at 1xg, with cultures in all matrix conditions displaying $\sim 95\%$ viability (Fig. 2). For EBs preserved with RNAlater II in μg , it was not possible to determine viability before automated injection of the preservative; however, since they were grown under identical conditions to the live-returned EBs, we expect similar viability.

Post- μg metabolic activity

Glucose present in the culture medium was measured immediately before launch and within 4 h of landing. Glucose concentration in μg and 1xg control bioreactors upon loading of EBs was identical (3.6 g/L). Following 15 days

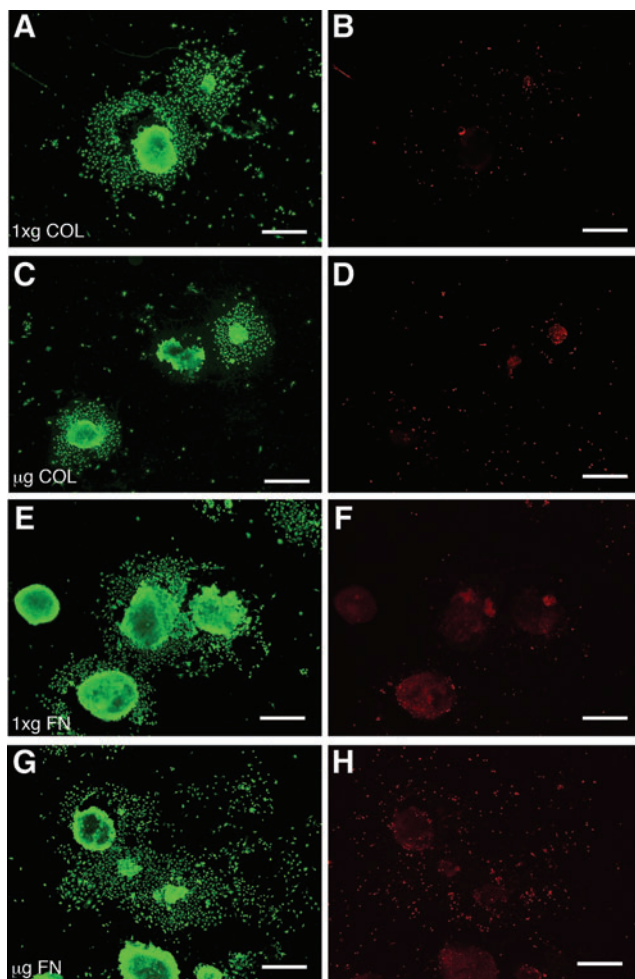


FIG. 2. Cells in EBs differentiated in μg showed no alterations in viability after 24 h outgrowth on either collagen or fibronectin matrices. Cell outgrowths from EBs adhering to collagen, COL (A–D) or fibronectin, FN (E–H) matrices 24 h following recovery from μg (C–D, G–H) and 1xg conditions (A–B, E–F) showed no significant differences in numbers of live viable cells (green fluorescence, calcein AM) or dead cells (red fluorescence, ethidium homodimer). Scale bar = 500 μm . 1xg, $n=5$; μg , $n=8$. Color images available online at www.liebertpub.com/scd

glucose concentration in μg bioreactors was on average 1.56 g/L, and 1.94 g/L in 1xg controls, indicating that EBs differentiated at 1xg consumed an average of 65.20% of glucose, while in μg EBs only consumed an average of 56.89% ($P < 0.01$). No significant alterations in lactate production were observed (15.96 and 17.96 mM average respectively, $P = 0.259$). Although production of lactate by EBs differentiated in μg was slightly lower than 1xg control production, both values are in a normal physiological range.

Post- μg cardiomyocyte differentiation

Following return to 1xg conditions, live EBs were placed on collagen or fibronectin matrices, and cells in EBs were allowed to migrate onto the ECM substrate for 9 days in an outgrowth assay. Cells in EBs still capable of outward migration are thought of being less differentiated and can provide a measure of the remaining earlier-stage progenitor or stem cell populations in EBs. In addition, during outgrowth new contractile cardiomyocyte colonies formed spontaneously, and were quantified to evaluate the remaining “stemness” of EBs following μg exposure. EBs differentiated in μg showed an average of 12.14 contractile colonies per 22 mm collagen matrix-coated coverslip, and 15.75 colonies on fibronectin, while ground controls only yielded an average of 7.77 and 6.08 colonies respectively ($P < 0.01$ and $P < 0.05$, Fig. 3). These results indicated that cells from post- μg EB outgrowths exhibited approximately twice the potential to differentiate into cardiomyocytes upon reloading at 1xg, as controls. This finding suggests that μg caused either a greater degree of stem cell pluripotency, greater numbers of stem cells, or a combination of both.

Microgravity embryoid body gene expression

To further investigate the hypothesis that EBs maintained greater stemness in μg , we conducted RT-qPCR on cells preserved on-orbit after 15 days in μg and analyzed over 250 genes of interest related to (1) ESC signaling and stem cell markers, (2) terminal, lineage-specific markers, and (3) the cell cycle and p53-signaling pathway. Automated on-orbit fixation ensured that any effects of reloading on the cells during orbiter reentry and landing were excluded. To determine the extent of differentiation, the gene expression profile of the 1xg control EBs was compared to that of the μg EBs and to the baseline undifferentiated mESCs. RT-qPCR gene arrays showed that out of 252 genes investigated, the majority showed two-fold or greater differences in expression level between EB differentiation-associated changes at 1xg compared to μg (Figs. 4–6, Table 1).

Gene expression alterations associated with stem cell signaling pathways. Growth in μg caused alterations in the Notch and Wnt stem cell signaling pathways including altered expression of NUMB (–2.45-fold, $P < 0.01$), DLL1 and DLL3 (1.67 and 3.85-fold respectively, $P < 0.5$), and DVL1 (–2.5-fold, $P < 0.01$) in EBs differentiated in μg compared to EBs differentiated at 1xg (Fig. 4A). Large increases in WNT1 were also found in μg samples compared to undifferentiated mESCs (81.91-fold, $P < 0.05$) and a smaller increase (not significant) in 1xg samples compared to undifferentiated mESCs (26.05-fold, $P = 0.091$). Decreased expression of FZD1 (–2.50-fold,

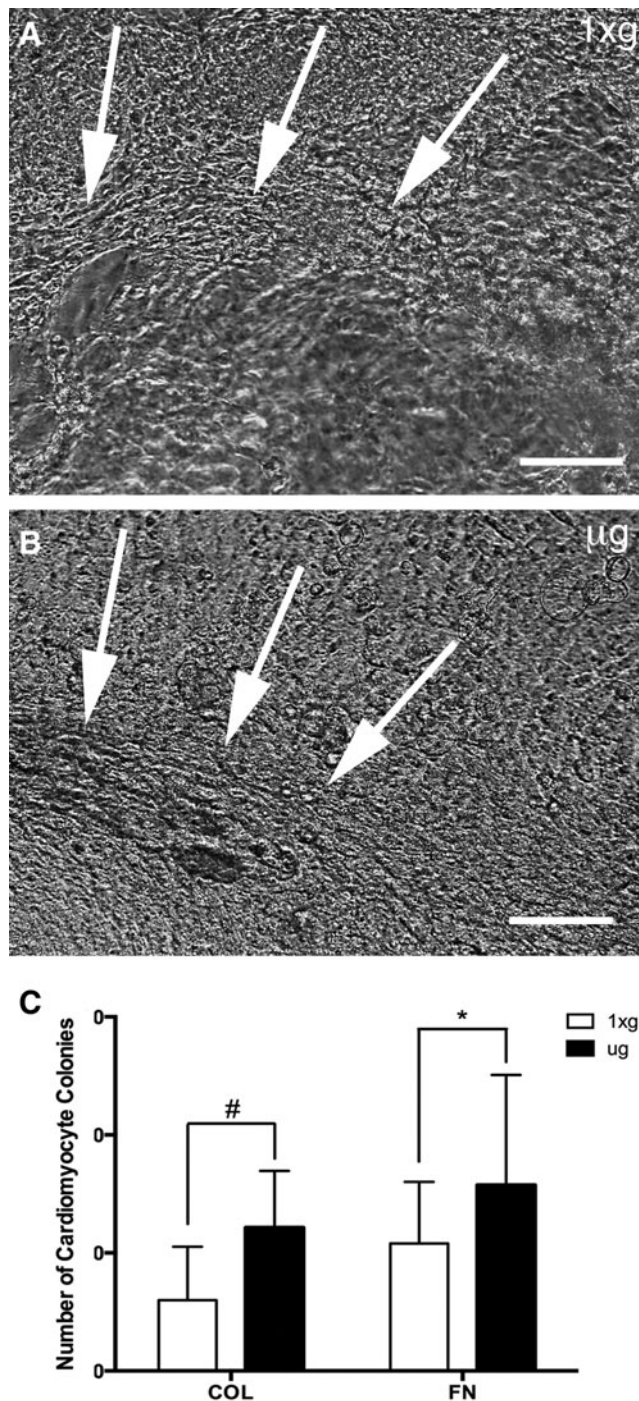


FIG. 3. EBs differentiated in μg showed increased differentiation potential following reloading at 1xg. Nine-day post- μg cell outgrowths from EBs differentiated in μg (**B**) showed increased numbers of contractile cardiomyocyte colonies (**C**) compared with ground control cultures (**A**). Arrows indicate contractile region of the EB outgrowth. Scale bar = 100 μm . 1xg, $n=5$; μg , $n=8$; # $P<0.01$, * $P<0.05$.

$P<0.01$) and ADAR (−1.70-fold, $P<0.01$) were also found in μg samples compared to 1xg controls.

Genes associated with the hematopoietic, mesenchymal, embryonic, and neural stem cell lineages were also investigated (Fig. 4B, Table 1). Microgravity downregulated a

number of ESC markers including KRT15 (−24.9-fold, $P<0.05$), FOXA2 (−1.7-fold, $P<0.01$), and PDX1 (−4.8-fold, $P<0.05$). EBs differentiated at 1xg had increased expression of ACTC1 compared with undifferentiated mESCs (22.48-fold, $P<0.01$), while μg samples showed a lower level of expression than 1xg controls (9.347, not significant), as did ASCL2 (−3.49 and −5.04 respectively, $P<0.01$, Fig. 4B, Table 1). Decreased expression of the hematopoietic stem cell marker CD3D was also observed in both 1xg and μg samples compared with undifferentiated mESCs (−1.53 and −1.77 respectively, $P<0.05$) and in MME (−5.50 and −5.02 respectively, $P<0.01$). Mesenchymal stem cell markers also showed significant alterations, including COL1A1 (−7.6-fold, $P<0.05$), PPAR γ (−7.0-fold, $P<0.05$), and COL9A1 (−20.2-fold, $P<0.05$, Fig. 4B, Table 1). The neural stem cell marker TUBB3 showed increased expression in μg samples compared with 1xg controls (5.9-fold, $P<0.05$, Fig. 4B, Table 1), and decreased expression of CD44 in μg samples compared with 1xg control (3.2-fold, $P<0.05$).

Gene expression alterations in stem cell properties. Stem cell-specific gene expression markers associated with cell division, self-renewal, adhesion, cell–cell communication, and metabolism were also investigated. The expression of several metabolic genes, including ALDH2, ABCG2, and FGFR1 decreased in 1xg controls compared with undifferentiated mESCs (−4.41, −4.06, and −2.42 respectively, $P<0.01$, Fig. 4C, Table 1). These genes also showed decreased expression in μg samples compared with undifferentiated mESCs (−3.14, −4.56, and −4.04 respectively, $P<0.01$) indicating that cell growth was not inhibited by spaceflight conditions. Expression of several cell adhesion molecules decreased in both μg - and 1xg-differentiated EBs compared with undifferentiated mESCs (Fig. 4C, Table 1). However, ACAN, an extracellular matrix protein in cartilaginous tissue, had increased expression in flight samples compared with ground samples and CDH2 had decreased expression. Furthermore, expression of NCAM1 and CD44 increased in 1xg samples compared with undifferentiated mESCs (3.01 and 5.30-fold change respectively, $P<0.01$) but their expression in μg -differentiated EBs did not change significantly compared to mESCs (2.034-fold change, $P=0.103$, and 1.629-fold change, $P=0.231$ respectively, Fig. 4C, Table 1). Significant alterations in cell–cell communication molecules (Fig. 4C, Table 1) were found. Specifically, GJB1 exhibited significantly decreased expression in μg samples (−65.49, $P<0.01$) compared with undifferentiated mESCs and compared directly to EBs differentiated at 1xg (−27.64, $P<0.01$). Growth factors and cytokines associated with stem cell differentiation, including IGF1, BMP2 and BMP3, and CXCL12 were found to be increased in EBs differentiated at 1xg compared with undifferentiated mESCs (30.25, 7.73, 7.38, and 6.77-fold respectively, $P<0.05$), but these had decreased expression in EBs differentiated in μg [4.30, 2.70, 5.33, and 2.47 (not significant) respectively, $P<0.05$, Fig. 4C]. Importantly, markers for stem cell self-renewal (eg, Neurog2, Sox1, and Sox2) were found to be decreased in EBs differentiated in normal 1xg conditions, while these markers were increased in EBs differentiated in μg conditions, possibly indicating that cells remained in a stem cell-like state rather than undergoing differentiation.

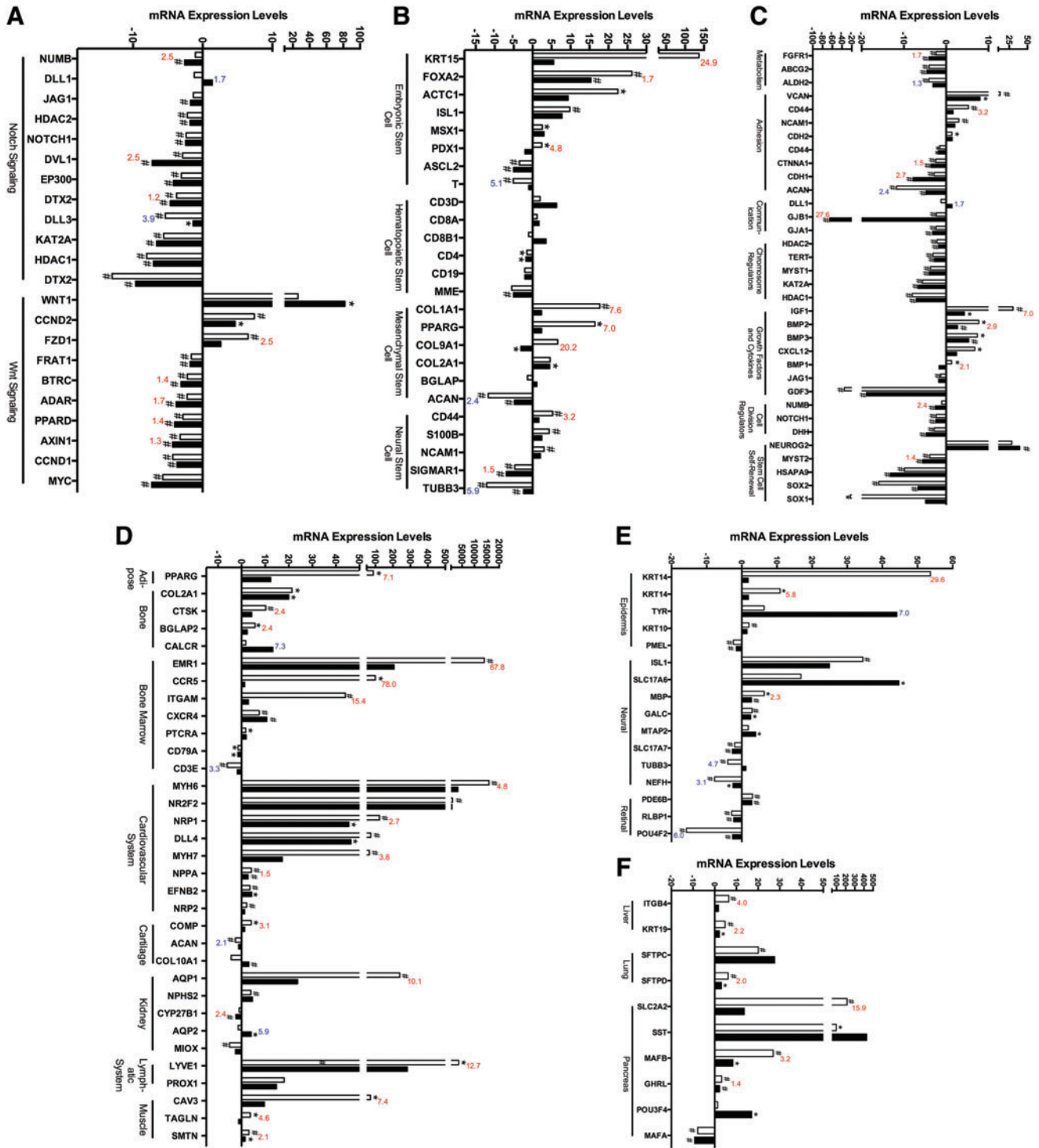


FIG. 4. EBs differentiated in μg showed altered expression of stem cell-specific markers and stem cell signaling molecules and decreased expression of terminal differentiation markers. Real time quantitative polymerase chain reaction (RT-qPCR) expression of EBs differentiated in μg showed alterations in genes associated with the Notch and Wnt stem cell signaling pathways (A), markers for stem cell lineages (B), and stem cell-specific markers for metabolism, adhesion, communication, and self-renewal (C). Furthermore, terminal differentiation markers showed significant alterations for all three germ layers—mesoderm (D), ectoderm (E), and endoderm (F). Bars indicate gene expression of 1xg- (white) and μg -differentiated (black) EBs compared to undifferentiated mESCs. Numbers indicate up- (blue) or downregulation (red) of the specified gene in μg samples compared to 1xg controls. $n=4$, $*P<0.05$, $\#P<0.01$. Color images available online at www.liebertpub.com/scd

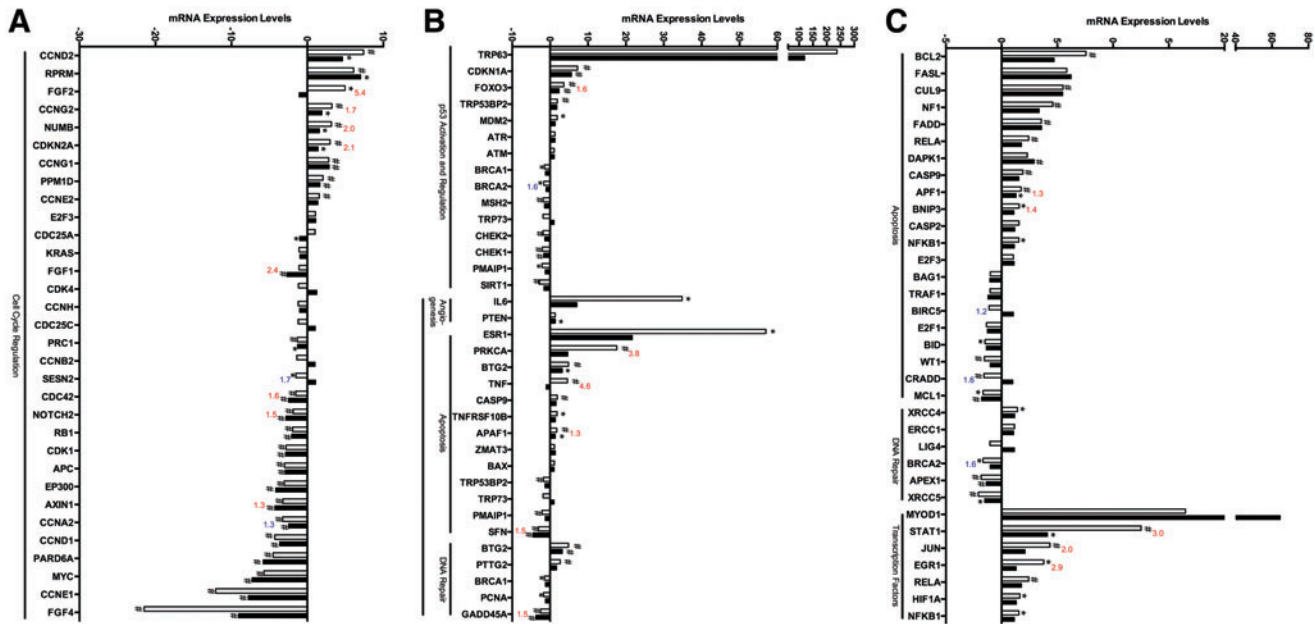


FIG. 5. Spaceflight altered the expression of genes associated with the cell cycle and p53 signaling pathway. RT-qPCR analysis of cells differentiated in μg showed key alterations in molecules associated with the cell cycle (A), activation and regulation of p53 and p53 targets (B), and p53 downstream responses (C). Bars indicate gene expression of 1xg- (white) and μg -differentiated (black) EBs compared to undifferentiated mESCs. Numbers indicate up- (blue) or downregulation (red) of the specified gene in μg samples compared to 1xg controls. $n=4$, * $P<0.05$, # $P<0.01$. Color images available online at www.liebertpub.com/scd

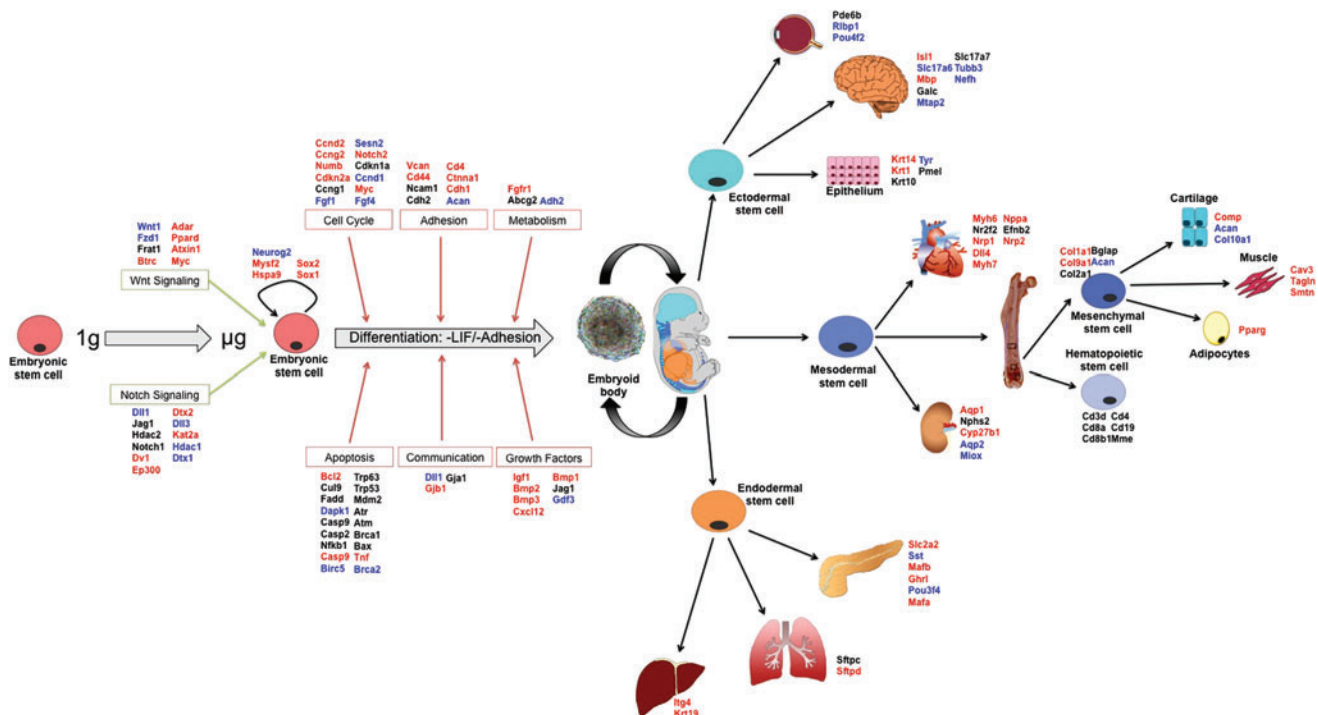


FIG. 6. Diagrammatic representation of gene expression results from STL1. Differentiation of EBs during μg revealed a broad downregulation in gene expression of both tissue-specific stem cell markers and terminal lineage differentiation markers. Furthermore, markers for stem cell signaling, cell cycle, adhesion, and growth factors were predominantly downregulated while most apoptosis markers remained unchanged in μg samples compared to controls. EBs differentiated in μg appeared to initiate the differentiation process but fail to express normal terminal differentiation markers expressed in mechanically loaded tissues. Blue indicates upregulation, red indicates downregulation, and black indicates no change. Color images available online at www.liebertpub.com/scd

TABLE 1. REAL TIME QUANTITATIVE POLYMERASE CHAIN REACTION ANALYSIS OF GENES ASSOCIATED WITH STEM CELL PLURIPOTENCY, LINEAGE DIFFERENTIATION, AND THE CELL CYCLE

Category	Symbol	mESC -> GC		mESC -> FLT		Changes in fold change of GC vs. FLT	GC -> FLT		
		Fold D	P value	Fold D	P value		Fold D	P value	
Stem cell-specific markers and stem cell signaling									
Signaling pathways	Notch	Dll1	-1.21	0.349	1.38	0.114	2.596	1.68	0.041
		Dll3	-5.36	<u>3.87E-05</u>	-1.38	<u>0.035</u>	3.975	3.87	<u>3.11E-04</u>
		Dtx1	-13.01	<u>3.88E-06</u>	-9.63	<u>3.68E-05</u>	3.379	1.35	0.406
		Dtx2	-3.75	<u>8.26E-07</u>	-4.65	<u>3.92E-07</u>	-0.904	-1.24	<u>0.010</u>
		Dvl1	-2.90	<u>1.19E-04</u>	-7.24	<u>3.84E-06</u>	-4.341	-2.50	<u>0.005</u>
		Ep300	-3.05	<u>1.31E-06</u>	-4.20	<u>4.54E-06</u>	-1.148	-1.38	0.054
		Hdac1	-8.04	<u>1.25E-06</u>	-7.08	<u>1.03E-07</u>	0.966	1.14	0.734
		Hdac2	-2.20	<u>9.23E-06</u>	-1.82	<u>0.001</u>	0.379	1.21	0.120
		Jag1	-1.33	0.050	-1.75	<u>0.002</u>	-0.418	-1.31	0.106
		Kat2a	-5.62	<u>7.56E-07</u>	-6.63	<u>1.39E-07</u>	-1.011	-1.18	0.314
	Wnt	Notch1	-2.38	<u>6.00E-04</u>	-2.46	<u>4.65E-06</u>	-0.077	-1.03	0.715
		Numb	-1.04	0.879	-2.59	<u>6.76E-05</u>	-1.546	-2.48	<u>0.002</u>
		Adar	-2.24	<u>4.74E-05</u>	-3.80	<u>6.04E-07</u>	-1.564	-1.70	<u>0.002</u>
		Axin1	-3.25	<u>6.26E-06</u>	-4.31	<u>2.76E-06</u>	-1.062	-1.33	<u>0.032</u>
		Btrc	-2.20	<u>1.13E-04</u>	-3.11	<u>1.85E-06</u>	-0.906	-1.41	<u>0.013</u>
		Ccnd1	-4.29	<u>8.01E-06</u>	-3.69	<u>5.76E-06</u>	0.606	1.16	0.467
		Ccnd2	7.41	<u>0.002</u>	4.64	<u>0.033</u>	-2.761	-1.59	0.168
		Frat1	-1.63	<u>0.002</u>	-1.80	<u>8.90E-05</u>	-0.169	-1.10	0.343
		Fzd1	6.51	<u>2.77E-04</u>	2.60	0.064	-3.909	-2.50	<u>0.005</u>
		Myc	-5.73	<u>0.001</u>	-7.32	<u>3.17E-04</u>	-1.592	-1.28	0.218
Stem cell differentiation marker	Embryonic cell lineage	Ppard	-2.83	<u>1.97E-05</u>	-4.04	<u>2.03E-05</u>	-1.205	-1.43	<u>0.029</u>
		Wnt1	26.05	0.091	81.91	<u>0.029</u>	55.857	3.14	0.065
		Actc1	22.48	<u>0.010</u>	9.35	0.093	-13.133	-2.41	0.358
		Ascl2	-3.49	<u>0.007</u>	-5.04	<u>0.005</u>	-1.548	-1.44	0.300
		Foxa2	26.18	<u>0.001</u>	15.37	<u>3.55E-04</u>	-10.818	-1.70	<u>0.022</u>
	Hematopoietic stem cells	Isl1	9.83	<u>0.001</u>	7.74	0.078	-2.082	-1.27	0.868
		Krt15	137.32	0.068	5.53	0.135	-131.783	-24.82	<u>0.038</u>
		Msx1	2.52	<u>0.029</u>	2.98	0.051	0.460	1.18	0.506
		Pdx1	2.42	<u>0.023</u>	-2.00	0.221	-4.417	-4.83	<u>0.006</u>
		T	-5.13	<u>0.001</u>	-1.00	0.840	4.127	5.11	<u>0.005</u>
Mesenchymal stem cells	Cd19	-2.06	0.141	-2.04	0.601	0.021	1.01	0.563	
	Cd3d	1.98	0.510	6.31	0.452	4.323	3.18	0.285	
	Cd4	-1.53	<u>0.043</u>	-1.77	<u>0.045</u>	-0.247	-1.16	0.468	
	Cd8a	1.17	0.353	1.67	0.366	0.503	1.43	0.358	
	Cd8b1	-1.05	0.950	3.51	0.422	4.566	3.70	0.352	
Neural stem cells	Mme	-5.49	<u>3.96E-06</u>	-5.02	<u>4.94E-06</u>	0.465	1.09	0.605	
	Acan	-11.72	<u>7.52E-09</u>	-4.80	<u>8.52E-06</u>	6.923	2.44	<u>0.011</u>	
	Bglap	-1.36	0.057	1.11	0.613	2.468	1.51	0.334	
	Col1a1	17.71	<u>0.006</u>	2.33	0.206	-15.378	-7.60	<u>0.012</u>	
	Col2a1	4.59	0.052	4.47	<u>0.027</u>	-0.114	-1.03	0.855	
Neural stem cells	Col9a1	6.59	0.087	-3.07	<u>0.042</u>	-9.662	-20.24	<u>0.036</u>	
	Pparg	16.44	<u>0.020</u>	2.35	0.179	-14.095	-7.01	<u>0.014</u>	
	Cd44	5.28	<u>1.12E-04</u>	1.63	0.231	-3.650	-3.24	<u>0.002</u>	
	Ncam1	3.01	<u>0.007</u>	2.03	0.103	-0.975	-1.48	0.245	
	S100b	4.36	<u>0.001</u>	2.41	0.138	-1.953	-1.81	0.111	
Neural stem cells	Sigmar1	-4.70	<u>1.99E-08</u>	-6.95	<u>6.27E-09</u>	-2.243	-1.48	<u>0.001</u>	
	Tubb3	-12.13	<u>1.94E-07</u>	-2.38	<u>3.03E-04</u>	9.747	5.09	<u>0.001</u>	

(continued)

TABLE 1. (CONTINUED)

Category	Symbol	mESC -> GC		mESC -> FLT		Changes in fold change of GC vs. FLT	GC -> FLT		
		Fold D	P value	Fold D	P value		Fold D	P value	
Stem cell-specific markers	Metabolic	Abcg2	-4.06	1.39E-07	-4.56	5.98E-08	-0.499	-1.12	0.208
		Aldh2	-4.10	1.47E-06	-3.11	2.88E-07	0.990	1.32	0.029
		Fgfr1	-2.42	1.90E-05	-4.04	2.04E-06	-1.621	-1.67	0.003
	Cell adhesion	Acan	-11.72	7.52E-09	-4.80	8.52E-06	6.923	2.44	0.011
		Cd4	-1.53	0.043	-1.77	0.045	-0.247	-1.16	0.468
		Cd44	5.28	1.12E-04	1.63	0.231	-3.650	-3.24	0.002
		Cdh1	-2.87	2.31E-05	-7.85	3.12E-07	-4.974	-2.73	0.001
		Cdh2	1.36	0.003	1.44	0.089	0.078	1.06	0.584
		Ctnna1	-2.51	2.24E-05	-3.63	6.44E-06	-1.124	-1.45	0.013
		Ncam1	3.01	0.007	2.03	0.103	-0.975	-1.48	0.245
		Vcan	12.47	0.001	7.99	0.023	-4.482	-1.56	0.217
	Cell-cell comms	Dll1	-1.21	0.349	1.38	0.114	2.596	1.68	0.041
		Gja1	-2.43	2.39E-05	-3.22	4.16E-05	-0.782	-1.32	0.102
		Gjb1	-2.37	0.002	-65.49	4.69E-09	-63.119	-27.64	0.002
	Chromosome regulators	Hdac1	-8.04	1.25E-06	-7.08	1.03E-07	0.966	1.14	0.734
		Hdac2	-2.20	9.23E-06	-1.82	0.001	0.379	1.21	0.120
		Kat2a	-5.62	7.56E-07	-6.63	1.39E-07	-1.011	-1.18	0.314
		Myst1	-3.74	2.91E-05	-4.03	2.82E-05	-0.291	-1.08	0.129
		Tert	-3.15	1.52E-04	-2.81	2.95E-04	0.342	1.12	0.374
	GF and cytokines	Bmp1	1.28	0.019	-1.66	0.071	-2.942	-2.13	0.005
		Bmp2	7.73	0.037	2.70	0.004	-5.031	-2.87	0.043
		Bmp3	7.38	0.039	5.33	0.002	-2.053	-1.39	0.217
		Cxcl12	6.77	0.014	2.47	0.140	-4.301	-2.74	0.055
		Gdf3	-35.19	2.47E-08	-18.90	2.09E-06	16.298	1.86	0.290
		Igf1	30.25	0.004	4.30	0.039	-25.956	-7.04	0.002
		Jag1	-1.33	0.050	-1.75	0.002	-0.418	-1.31	0.106
		Dhh	-2.84	0.013	-4.71	0.004	-1.872	-1.66	0.070
Regulation cell division	Notch1	-2.38	0.001	-2.46	4.65E-06	-0.077	-1.03	0.715	
	Numb	-1.04	0.879	-2.59	6.76E-05	-1.546	-2.48	0.002	
Self-renewal	Hspa9	-9.89	3.77E-06	-13.22	2.61E-06	-3.321	-1.34	0.160	
	Myst2	-3.88	3.69E-08	-5.60	1.22E-07	-1.713	-1.44	0.007	
	Neurog2	28.34	0.091	39.30	0.006	10.961	1.39	0.438	
	Sox1	-22.94	0.034	-4.85	0.076	18.090	4.73	0.096	
	Sox2	-15.95	7.56E-08	-6.67	1.18E-05	9.278	2.39	0.063	
Terminal differentiation markers									
Ectoderm	Epidermal	Krt1	10.91	0.031	1.90	0.092	-9.015	-5.75	0.019
		Krt10	2.01	0.010	1.48	0.168	-0.537	-1.36	0.208
		Krt14	53.67	0.070	1.82	0.232	-51.852	-29.55	0.038
		Pmel	-2.39	2.50E-04	-1.55	0.00E+00	0.842	1.54	0.010
		Tyr	6.34	0.085	44.12	0.059	37.784	6.96	0.049
	Neural	Galc	2.97	2.24E-04	2.55	0.026	-0.413	-1.16	0.514
		Isl1	34.46	0.002	24.94	0.050	-9.520	-1.38	0.891
		Mbp	6.41	0.013	2.77	0.003	-3.639	-2.32	0.025
		Mtap2	1.85	0.194	3.98	0.021	2.123	2.15	0.125
		Nefh	-7.75	0.001	-2.50	0.011	5.250	3.10	0.015
		Slc17a6	16.85	0.185	44.69	0.032	27.844	2.65	0.478
		Slc17a7	-2.03	0.008	-2.67	0.002	-0.643	-1.32	0.189
		Tubb3	-4.01	2.59E-04	1.18	0.236	5.192	4.74	0.001
	Retina	Pde6b	3.08	2.19E-04	2.85	4.84E-04	-0.231	-1.08	0.400
		Pou4f2	-15.77	2.24E-04	-2.62	0.003	13.150	6.01	0.001
		Rlbp1	-2.88	4.31E-05	-2.30	0.008	0.581	1.25	0.310

(continued)

TABLE 1. (CONTINUED)

Category	Symbol	mESC -> GC		mESC -> FLT		Changes in fold change of GC vs. FLT	GC -> FLT		
		Fold D	P value	Fold D	P value		Fold D	P value	
Mesoderm	Adipose	Pparg	87.81	0.018	12.34	0.069	-75.473	-7.12	0.015
	Bone	Bglap2	5.64	0.013	2.39	0.124	-3.250	-2.36	0.046
		Calcr	1.82	0.064	13.22	0.008	11.402	7.27	0.004
		Col2a1	21.35	0.028	19.96	0.018	-1.386	-1.07	0.837
	Bone marrow	Ctsk	10.22	0.002	4.28	0.111	-5.945	-2.39	0.044
		Ccr5	99.34	0.020	1.27	0.584	-98.064	-77.98	0.007
		Cd3e	-6.12	0.001	-1.87	0.093	4.252	3.28	0.040
		Cd79a	-1.50	0.049	-1.59	0.012	-0.091	-1.06	0.723
		Cxcr4	7.45	0.009	10.71	0.007	3.256	1.44	0.193
		Emr1	14032.47	0.004	206.73	0.231	-13825.75	-67.88	0.001
		Itgam	44.03	0.007	2.86	0.149	-41.167	-15.39	0.003
		Ptcr	1.76	0.029	1.93	0.305	0.174	1.10	0.560
	Cardiovascular system	Dll4	73.47	0.001	46.41	0.018	-27.056	-1.58	0.190
		Efnb2	3.55	9.10E-05	4.28	0.023	0.731	1.21	0.336
		Myh6	15902.77	1.65E-04	3284.04	0.056	-12618.731	-4.84	0.014
		Myh7	65.37	0.002	17.24	0.109	-48.128	-3.79	0.049
		Nppa	4.11	0.002	2.71	0.002	-1.407	-1.52	0.034
		Nr2f2	1093.35	0.010	871.36	0.065	-221.988	-1.25	0.900
		Nrp1	122.98	8.61E-05	45.49	0.048	-77.493	-2.70	0.017
		Nrp2	2.15	1.57E-04	1.28	0.352	-0.865	-1.67	0.076
	Cartilage	Acan	-2.63	1.90E-05	-1.26	0.294	1.369	2.08	0.017
		Col10a1	-4.46	0.210	3.06	0.003	7.511	13.61	0.470
		Comp	4.05	0.013	1.30	0.286	-2.749	-3.12	0.009
	Kidney	Aqp1	239.71	0.002	23.74	0.077	-215.964	-10.10	0.001
		Aqp2	-1.45	0.371	4.07	0.048	5.520	5.91	0.012
		Cyp27b1	-1.02	0.887	-2.43	0.007	-1.409	-2.39	0.003
		Miox	-5.12	1.55E-04	-2.57	0.373	2.542	1.99	0.262
Nphs2		3.94	2.85E-04	4.59	0.135	0.659	1.17	0.503	
Lymphatic	Lyve1	3601.94	0.018	282.89	0.148	-3319.046	-12.73	0.012	
	Prox1	18.02	0.001	14.74	0.008	-3.283	-1.22	0.494	
Muscle	Cav3	71.64	0.018	9.65	0.154	-61.996	-7.43	0.020	
	Smtn	3.10	0.001	1.47	0.049	-1.631	-2.11	0.002	
	Tagln	3.66	0.017	-1.26	0.971	-4.915	-4.60	0.009	
Endoderm	Liver	Itgb4	6.47	0.010	1.75	0.052	-4.716	-3.69	0.007
		Krt19	4.77	1.53E-05	2.18	0.047	-2.584	-2.18	0.002
	Lung	Sftpc	20.10	0.002	27.63	0.164	7.536	1.37	0.414
		Sftpd	6.18	0.006	3.11	0.020	-3.069	-1.99	0.030
	Pancreas	Ghrl	3.21	3.75E-05	2.25	0.002	-0.955	-1.42	0.006
		Mafa	-7.83	5.88E-05	-9.28	3.37E-05	-1.445	-1.18	0.367
		Mafb	26.96	4.39E-06	8.36	0.019	-18.604	-3.23	2.46E-04
		Pou3f4	1.36	0.233	17.03	0.044	15.674	12.52	0.692
		Slc2a2	215.52	0.001	13.60	0.089	-201.920	-15.85	4.22E-04
		Sst	98.51	0.044	429.62	0.105	331.107	4.36	0.105
p53 signaling	Cell cycle regulation	Apc	-3.01	2.02E-05	-2.95	2.18E-05	0.066	1.02	0.607
p53 and cell cycle		Axin1	-3.25	6.26E-06	-4.31	2.76E-06	-1.062	-1.33	0.032
		Ccna2	-3.25	2.25E-06	-2.50	5.31E-05	0.750	1.30	0.038
		Ccnb2	-1.39	0.166	1.03	0.734	2.415	1.42	0.104
		Ccnd1	-4.29	8.01E-06	-3.69	5.76E-06	0.606	1.16	0.467
		Ccnd2	7.41	0.002	4.64	0.033	-2.761	-1.59	0.168
		Ccne1	-12.07	1.73E-10	-7.80	3.68E-07	4.269	1.55	0.061
		Ccne2	1.57	2.60E-05	1.39	0.071	-0.179	-1.13	0.337
		Ccng1	2.80	0.003	2.90	0.005	0.104	1.04	0.771
		Ccng2	3.24	2.44E-04	1.95	0.018	-1.291	-1.66	0.007
		Ccnh	-1.20	0.042	-1.06	0.502	0.143	1.14	0.163

(continued)

TABLE 1. (CONTINUED)

Category	Symbol	mESC -> GC		mESC -> FLT		Changes in fold change of GC vs. FLT	GC -> FLT		
		Fold D	P value	Fold D	P value		Fold D	P value	
	Cdc25a	1.01	0.874	-1.05	0.689	-2.061	-1.06	0.652	
	Cdc25c	-1.21	0.267	1.06	0.397	2.274	1.29	0.105	
	Cdc42	-1.53	0.001	-2.50	3.61E-05	-0.964	-1.63	0.003	
	Cdk1	-2.79	8.32E-07	-2.89	0.000	-0.095	-1.03	0.521	
	Cdk4	-1.17	0.579	1.27	0.316	2.443	1.49	0.143	
	Cdkn2a	2.98	0.008	1.43	0.044	-1.545	-2.08	0.010	
	E2f3	1.06	0.702	1.13	0.594	0.072	1.07	0.768	
	Ep300	-3.05	1.31E-06	-4.20	4.54E-06	-1.148	-1.38	0.054	
	Fgf1	-1.11	0.509	-2.72	0.003	-1.604	-2.44	0.007	
	Fgf2	4.96	0.026	-1.09	0.917	-6.051	-5.43	0.010	
	Fgf4	-21.49	5.33E-07	-9.10	4.56E-05	12.385	2.36	0.169	
	Kras	-1.10	0.768	-1.00	0.895	0.098	1.10	0.711	
	Myc	-5.73	0.001	-7.32	3.17E-04	-1.592	-1.28	0.218	
	Notch2	-1.89	2.72E-04	-2.85	2.77E-07	-0.959	-1.51	0.005	
	Numb	3.16	0.001	1.61	0.029	-1.552	-1.96	0.002	
	Pard6a	-4.51	2.58E-06	-5.85	8.41E-07	-1.342	-1.30	0.110	
	Ppm1d	2.07	0.004	1.68	0.001	-0.391	-1.24	0.076	
	Prc1	-1.33	0.003	-1.32	0.023	0.005	1.01	0.898	
	Rb1	-1.93	0.005	-2.09	0.005	-0.158	-1.08	0.552	
	Rprm	6.10	0.007	7.05	0.016	0.945	1.16	0.501	
	Sesn2	-1.52	0.029	1.10	0.527	2.616	1.67	0.041	
p53 activation and regulation	Atm	1.05	0.688	1.05	0.628	0.003	-1.00	0.923	
	Atr	1.24	0.267	1.25	0.173	0.006	1.00	0.965	
	Brca1	-1.51	0.046	-1.18	0.282	0.331	1.28	0.125	
	Brca2	-1.67	0.011	-1.04	0.752	0.632	1.61	0.011	
	Cdkn1a	7.22	1.41E-04	5.61	0.005	-1.611	-1.29	0.205	
	Chek1	-2.07	4.89E-04	-1.68	0.001	0.391	1.23	0.113	
	Chek2	-1.89	0.026	-1.37	0.281	0.524	1.38	0.291	
	Foxo3	3.63	9.00E-06	2.34	3.26E-04	-1.292	-1.55	2.63E-04	
	Mdm2	1.87	0.021	1.29	0.216	-0.576	-1.45	0.091	
	Msh2	-1.83	0.002	-1.46	0.059	0.375	1.26	0.235	
	Pmaip1	-2.14	0.018	-1.26	0.256	0.882	1.70	0.111	
	Sirt1	-2.87	0.004	-1.61	0.226	1.264	1.79	0.170	
	Trp53bp2	1.89	0.010	1.74	0.056	-0.153	-1.09	0.728	
	Trp63	236.98	0.054	119.58	0.141	-117.396	-1.98	0.390	
	Trp73	-1.87	0.152	1.01	0.812	2.878	1.88	0.182	
Target	Angiogenesis	Il6	34.83	0.021	7.03	0.224	-27.795	-4.95	0.051
		Pten	1.34	0.061	1.35	0.038	0.005	1.00	0.992
	Apoptosis	Apaf1	1.75	1.13E-04	1.32	0.042	-0.432	-1.33	0.006
		Bax	1.11	0.297	1.03	0.597	-0.082	-1.08	0.342
		Btg2	4.86	0.005	3.15	0.012	-1.707	-1.54	0.092
		Casp9	1.91	0.003	1.56	0.125	-0.349	-1.22	0.390
		Esr1	56.92	0.025	21.67	0.161	-35.250	-2.63	0.222
		Pmaip1	-2.14	0.018	-1.26	0.256	0.882	1.70	0.111
		Prkca	17.59	0.001	4.60	0.101	-12.994	-3.83	0.004
		Sfn	-3.09	1.03E-04	-4.53	1.05E-05	-1.439	-1.47	0.043
		Tnf	4.57	0.003	-1.02	0.650	-5.586	-4.64	0.046
		Tnfrsf10b	1.83	0.016	1.36	0.167	-0.468	-1.34	0.149
		Trp53	-1.81	0.001	-1.32	0.137	0.489	1.37	0.105
		Trp73	-1.87	0.152	1.01	0.812	2.878	1.88	0.182
		Zmat3	1.13	0.447	1.34	0.266	0.208	1.18	0.436
	DNA repair	Brca1	-1.51	0.046	-1.18	0.282	0.331	1.28	0.125
		Btg2	4.86	0.005	3.15	0.012	-1.707	-1.54	0.092
		Gadd45a	-2.54	2.00E-06	-3.76	5.55E-07	-1.216	-1.48	0.003
		Pcna	-1.74	0.016	-1.18	0.082	0.563	1.48	0.057
		Pttg1	2.66	0.001	1.67	0.148	-0.989	-1.59	0.085

(continued)

TABLE 1. (CONTINUED)

Category	Symbol	mESC → GC		mESC → FLT		Changes in fold change of GC vs. FLT	GC → FLT		
		Fold D	P value	Fold D	P value		Fold D	P value	
Downstream	Apoptosis	Apaf1	<i>1.75</i>	<i>1.13E-04</i>	<i>1.32</i>	<i>0.042</i>	<i>-0.432</i>	<i>-1.33</i>	<i>0.006</i>
		Bag1	<i>-1.01</i>	<i>0.982</i>	<i>-1.07</i>	<i>0.786</i>	<i>-0.058</i>	<i>-1.05</i>	<i>0.792</i>
		Bcl2	<i>7.57</i>	<i>0.005</i>	<i>4.73</i>	<i>0.085</i>	<i>-2.839</i>	<i>-1.60</i>	<i>0.297</i>
		Bid	<i>-1.49</i>	<i>0.037</i>	<i>-1.39</i>	<i>0.112</i>	<i>0.104</i>	<i>1.08</i>	<i>0.669</i>
		Birc5	<i>-1.13</i>	<i>0.164</i>	<i>1.07</i>	<i>0.254</i>	<i>2.197</i>	<i>1.21</i>	<i>0.046</i>
		Bnip3	<i>1.57</i>	<i>0.011</i>	<i>1.12</i>	<i>0.127</i>	<i>-0.453</i>	<i>-1.40</i>	<i>0.011</i>
		Casp2	<i>1.55</i>	<i>0.084</i>	<i>1.20</i>	<i>0.428</i>	<i>-0.354</i>	<i>-1.30</i>	<i>0.342</i>
		Casp9	<i>1.91</i>	<i>0.003</i>	<i>1.56</i>	<i>0.125</i>	<i>-0.349</i>	<i>-1.22</i>	<i>0.390</i>
		Cradd	<i>-1.59</i>	<i>0.004</i>	<i>1.02</i>	<i>0.774</i>	<i>2.607</i>	<i>1.62</i>	<i>0.003</i>
		Cul9	<i>5.51</i>	<i>0.002</i>	<i>5.49</i>	<i>0.060</i>	<i>-0.025</i>	<i>-1.00</i>	<i>0.729</i>
		Dapk1	<i>2.30</i>	<i>0.062</i>	<i>2.93</i>	<i>0.009</i>	<i>0.629</i>	<i>1.27</i>	<i>0.416</i>
		E2f1	<i>-1.36</i>	<i>0.422</i>	<i>-1.29</i>	<i>0.340</i>	<i>0.075</i>	<i>1.06</i>	<i>0.971</i>
		E2f3	<i>1.06</i>	<i>0.702</i>	<i>1.13</i>	<i>0.594</i>	<i>0.072</i>	<i>1.07</i>	<i>0.768</i>
		Fadd	<i>3.56</i>	<i>0.001</i>	<i>3.61</i>	<i>0.170</i>	<i>0.047</i>	<i>1.01</i>	<i>0.662</i>
		Fasl	<i>5.83</i>	<i>0.055</i>	<i>6.26</i>	<i>0.207</i>	<i>0.425</i>	<i>1.07</i>	<i>0.688</i>
	Mcl1	<i>-1.66</i>	<i>0.029</i>	<i>-1.82</i>	<i>0.009</i>	<i>-0.158</i>	<i>-1.09</i>	<i>0.647</i>	
	Nf1	<i>4.59</i>	<i>0.004</i>	<i>3.40</i>	<i>0.080</i>	<i>-1.193</i>	<i>-1.35</i>	<i>0.472</i>	
	Nfkb1	<i>1.54</i>	<i>0.036</i>	<i>1.15</i>	<i>0.355</i>	<i>-0.392</i>	<i>-1.34</i>	<i>0.119</i>	
	Rela	<i>2.43</i>	<i>0.001</i>	<i>1.79</i>	<i>0.077</i>	<i>-0.637</i>	<i>-1.36</i>	<i>0.169</i>	
	Traf1	<i>-1.03</i>	<i>0.979</i>	<i>-1.24</i>	<i>0.903</i>	<i>-0.209</i>	<i>-1.20</i>	<i>0.881</i>	
	Wt1	<i>-1.55</i>	<i>0.003</i>	<i>-1.04</i>	<i>0.821</i>	<i>0.512</i>	<i>1.49</i>	<i>0.240</i>	
	DNA repair	Apex1	<i>-1.84</i>	<i>0.004</i>	<i>-1.39</i>	<i>0.002</i>	<i>0.449</i>	<i>1.32</i>	<i>0.096</i>
		Brca2	<i>-1.67</i>	<i>0.011</i>	<i>-1.04</i>	<i>0.752</i>	<i>0.632</i>	<i>1.61</i>	<i>0.011</i>
		Ercc1	<i>1.15</i>	<i>0.077</i>	<i>1.10</i>	<i>0.338</i>	<i>-0.053</i>	<i>-1.05</i>	<i>0.634</i>
		Lig4	<i>-1.05</i>	<i>0.970</i>	<i>1.17</i>	<i>0.454</i>	<i>2.216</i>	<i>1.23</i>	<i>0.450</i>
		Xrcc4	<i>1.42</i>	<i>0.010</i>	<i>1.18</i>	<i>0.103</i>	<i>-0.238</i>	<i>-1.21</i>	<i>0.082</i>
		Xrcc5	<i>-2.08</i>	<i>0.001</i>	<i>-1.54</i>	<i>0.010</i>	<i>0.541</i>	<i>1.35</i>	<i>0.064</i>
	TF	Egr1	<i>3.78</i>	<i>0.027</i>	<i>1.31</i>	<i>0.467</i>	<i>-2.466</i>	<i>-2.87</i>	<i>0.049</i>
		Hif1a	<i>1.64</i>	<i>0.026</i>	<i>1.33</i>	<i>0.104</i>	<i>-0.309</i>	<i>-1.24</i>	<i>0.217</i>
		Jun	<i>4.33</i>	<i>0.002</i>	<i>2.12</i>	<i>0.076</i>	<i>-2.210</i>	<i>-2.04</i>	<i>0.019</i>
Myod1		<i>16.49</i>	<i>0.167</i>	<i>64.58</i>	<i>0.122</i>	<i>48.086</i>	<i>3.92</i>	<i>0.222</i>	
Nfkb1		<i>1.54</i>	<i>0.036</i>	<i>1.15</i>	<i>0.355</i>	<i>-0.392</i>	<i>-1.34</i>	<i>0.119</i>	
Rela		<i>2.43</i>	<i>0.001</i>	<i>1.79</i>	<i>0.077</i>	<i>-0.637</i>	<i>-1.36</i>	<i>0.169</i>	
Stat1		<i>12.52</i>	<i>0.002</i>	<i>4.13</i>	<i>0.017</i>	<i>-8.389</i>	<i>-3.03</i>	<i>0.005</i>	

Bold italics indicates upregulation, *bold* indicates downregulation and *italics* indicates no significant biological change of test samples compared to controls in each respective column (GC vs. mESCs, FLT vs. mESCs, FLT vs. GC). Highlighting indicates net downregulation (*dark gray*), upregulation (*gray*) or no change (*light gray*) in fold change of μ g and 1xg controls compared to undifferentiated mESCs. *Bold underlined* indicates significant change ($P < 0.05$).

1xg, Earth's gravity; mESC, mouse embryonic stem cell; GC, ground control; FLT, spaceflight.

Gene expression of terminal lineage differentiation markers. To further investigate the effects of spaceflight on differentiation into multiple cell lineages, we conducted RT-qPCR analysis of terminal lineage differentiation markers from the three germ layers—mesoderm, endoderm, and ectoderm. We specifically investigated genes associated with terminal differentiation of adipose, bone, bone marrow, cardiovascular, cartilage, kidney, lymphatic, and muscle tissues. The adipose tissue marker PPAR γ was downregulated in EBs differentiated in μ g conditions compared with 1xg controls (-7.12 , $P < 0.05$). COL2A1 showed similar levels of expression in 1xg controls and μ g samples compared to undifferentiated mESCs (19.96 and 21.25-fold respectively, $P < 0.05$), however, expression of CTSK and BGLAP were significantly decreased in μ g samples (-2.93 and -2.36 -fold respectively, $P < 0.05$, Fig. 4D). CALCR was increased in EBs differenti-

ated in μ g conditions compared with 1xg controls (7.27, $P < 0.01$, Fig. 4D). Importantly, markers for immune cells including EMR1, CCR5, and ITGAM were significantly downregulated in microgravity samples compared with 1xg controls (-67.88 , -77.98 , and -15.39 -fold respectively, $P < 0.01$, Fig. 4D, Table 1). We also found decreases in a number of cardiovascular differentiation markers. Specifically, cardiomyocyte markers (MYH6 and MYH7), arterial endothelium markers (NRP1), and lymphatic endothelial markers (LYVE1) were downregulated in EBs differentiated in μ g compared with 1xg (-4.84 , -3.79 , -2.70 , and -12.73 -fold respectively, $P < 0.05$). DLL4, exhibited significant increases in μ g and 1xg samples compared with undifferentiated mESCs (73.47 and 46.41-fold respectively, $P < 0.05$), however, the increase in expression for the μ g samples was less than the increases in 1xg controls and compared with levels in

undifferentiated mESCs. The cartilage specific differentiation marker, COMP was also altered in μg samples compared to 1xg controls (-3.12 , $P < 0.01$). COL10A1 exhibited increased expression in EBs differentiated in μg samples compared with undifferentiated mESCs (3.06-fold, $P < 0.01$), however, no significant differences were found when compared to EBs differentiated at 1xg (Table 1). We also found decreased expression in kidney markers AQP1 and CYP27B1 (-10.1 and -2.39 -fold respectively, $P < 0.01$). On the other hand, AQP2 had increased expression in μg samples compared with 1xg controls (5.91, $P < 0.05$, Fig. 4D). Investigation into terminal muscle lineage markers resulted in decreased expression of CAV3 (-7.4 -fold, $P < 0.05$), TAGLN (-4.6 -fold, $P < 0.05$), and SMTN (-2.1 -fold, $P < 0.05$) in EBs differentiated in μg compared with 1xg controls (Fig. 4D).

Significant alterations in differentiation of tissues from the ectoderm and endoderm germ layers also were observed in EBs differentiated in μg conditions (Figs. 4 and 6). Specifically, epidermal lineage markers including KRT1, 14, and 15, were downregulated (-5.75 , -29.55 , and -24.9 -fold, $P < 0.05$, Fig. 4E) while expression of PMEL, a protein expressed in pigment cells, was upregulated in μg differentiated EBs (1.5-fold, $P < 0.01$, Fig. 4E). The retinal ganglion cell marker, POU4F2 was increased in μg -differentiated EBs compared with 1xg controls (6.01-fold, $P < 0.01$, Table 1). Markers for neural tissue differentiation showed increased expression in μg samples compared with 1xg controls. Specifically, the expression of two markers for mature neurons, TUBB3 and NEFH, showed increased expression in μg -differentiated EBs compared with 1xg controls (4.74 and 3.10-fold change respectively, $P < 0.05$, Fig. 4E). Markers for cholangiocytes, found in the liver, were also downregulated in μg samples, including ITGB4 (-3.69 , $P < 0.01$) and KRT19 (-2.18 , $P < 0.01$), as were markers for pancreatic cells, including SLC2A2 (-15.85 , $P < 0.01$), MAFB (-3.23 , $P < 0.01$), and GHRL (-1.42 , $P < 0.01$), as seen in Fig. 4F.

Collectively, these results indicate that the expression of lineage-specific markers during differentiation at 1xg, fail to appear normally in μg , suggesting that stem cells in EBs did not fully differentiate under mechanically unloaded conditions.

Gene expression analysis of the cell cycle and p53 signaling pathway. Genes associated with cell cycle regulation and the p53 signaling pathway were then investigated, to determine whether μg reduced cell proliferation and increased apoptosis or cell cycle arrest (Fig. 5). In control/1xg conditions, stem cells differentiated into EBs showed downregulation of cell cycle genes possibly associated with differentiation. Specifically, mESCs differentiated into EBs at 1xg, showed increased expression of CDKN1a (7.22-fold, $P < 0.01$). Although EBs differentiated in μg showed similar cell cycle arrest increase trends, the level of expression of cell cycle genes in μg was lower than that of 1xg controls, indicating greater proliferation potential (Fig. 5). We found, however, no significant alterations in TRP53 in EBs differentiated in μg versus 1xg, suggesting that apoptosis was not significantly changed at the time of fixation (Table 1). Furthermore, we also found no significant alterations in radiation response genes ATM and ATR (Fig. 5, Table 1). Upregulation of some apoptosis-related genes was observed in EBs differentiated at 1xg relative to undifferentiated mESCs, including BCL2 (7.57-fold, $P < 0.01$), CUL9 (5.51, $P < 0.01$), FADD (3.56, $P < 0.01$), RELA (2.43, $P < 0.01$), and CASP9 (1.91, $P < 0.01$,

Fig. 5). DAPK1, on the other hand, displayed increased expression in EBs differentiated in μg compared with undifferentiated mESCs (2.93, $P < 0.01$). These, however, were not significantly changed between 1xg and μg , and therefore their elevation of expression may be due to normal levels of apoptosis occurring during differentiation. Some p53 target genes showed increased expression in EBs differentiated at 1xg but not in EBs differentiated in μg compared to undifferentiated mESCs, including ESR1, PRKC α , and TNF (56.92, 17.59, 4.86 respectively, $P < 0.05$, Fig. 5). Finally, several downstream transcription factors also showed downregulation in μg samples compared with 1xg controls, including STAT1, JUN, and EGR1 (-3.03 , -2.04 , and -2.87 -fold respectively, $P < 0.05$, Fig. 5).

Discussion

In this study we investigated in vitro differentiation of mESC cultures in μg , to quantify the role and importance of gravity-generated forces on earth in promoting stem cell-based tissue regenerative health. Spaceflight in μg is known to cause tissue degeneration in mammals via complex mechanisms that include active tissue degradation, but also, we hypothesize, by the arrest of stem cell-based tissue regeneration. Here, we focused on the mechanism of regenerative arrest due to mechanical unloading. We show that exposure to microgravity during spaceflight preserved progenitor stemness and inhibited the expression of terminal differentiation markers for tissues derived from all three primary germ layers.

Previous studies of ESCs using experimental models that simulate microgravity, such as RPM and RWV, have shown varied outcomes including decreased cell numbers associated with increased apoptosis, altered adhesion properties, and differentiation [10]. In contrast, following 15 days differentiation in actual μg , EBs had similar viability levels to those of 1xg controls, and similar matrix adhesion to fibronectin and collagen. EBs differentiated in μg appeared to consume slightly less glucose than those differentiated at 1xg, suggesting reduced cell number, mass, or reduced metabolic rate.

To further determine the effects of μg unloading on cell proliferation and apoptosis in EBs, genes associated with the cell cycle and the p53-signaling pathway were investigated. We found no alterations in the expression of majority of apoptosis-related genes, including p53, p53-regulating genes, and genes involved in p53 activation, suggesting unaltered levels of apoptosis. Similar upregulation of expression of some apoptosis-related genes was observed in both μg samples and 1xg controls relative to undifferentiated mESCs, and may be due to normal apoptosis during differentiation, such as occurs during digit development. Apoptosis may also occur inside EBs as they enlarge and the center of cell masses becomes anoxic and nutrient deprived due to lack of vascularization [21], or in cells that fail to adhere to EB masses. Because only initial undifferentiated mESCs and terminal samples of differentiation cultures were collected, it is formally possible that differential apoptosis may have occurred initially, resulting in decreases in cell number and therefore decreased glucose consumption. In fact, μg altered the expression of cyclins that control cell cycle progression (eg, CCNA2, CCND1, and CCNG2), suggesting a decrease in

proliferation. Although no alterations were seen in CDKs, increased expression of CDKN1a/p21 in both μg - and 1xg-differentiated EBs was observed, however, expression of CDKN1a/p21 in μg samples was significantly less than that of 1xg controls. CDKN1a/p21 upregulation can occur in arrest of cell cycle for differentiation, in response to cell irradiation resulting in DNA damage, in response to oxidative damage, or in senescent cells [22–27]. As EBs differentiated at 1xg exhibited significantly increased expression of most terminal lineage markers that failed to appear to the same extent in μg samples, decreased expression of CDKN1A/p21 in μg samples compared with 1xg controls may be further evidence for decreased differentiation of EBs in μg . FGF1, which inhibits apoptosis and cell cycle arrest and also plays a role in embryonic development, was downregulated in μg samples, while FGF4, which promotes proliferation of mESCs [28], exhibited increased expression in μg -differentiated EBs compared with 1xg-differentiated EBs. Collectively, these gene expression data provide evidence for the hypothesis that cell cycle arrest occurs in EBs exposed to μg without the corresponding cell differentiation, possibly causing accumulation of partially differentiated cells ready for differentiation upon reloading.

To further characterize both the adhesion capacity and differentiation of EBs after reloading, we continued μg -exposed EB cultures on earth at 1 g for 9 days and quantified the differentiation of contractile cardiomyocytes as a method of evaluating differentiation [12,15,29]. Increased numbers of beating cardiomyocyte clusters in post- μg culture and decreased expression of cardiomyocyte markers suggest that EBs differentiated in μg retained more stem cells and overall greater pluripotency as a result of not progressing normally through differentiation as seen in loaded 1xg control samples. Similar results have been seen in our bone marrow stem cell differentiation experiments in μg -exposed mice that resulted in increased osteoclastogenesis and osteoblastogenesis potential following reloading at 1xg [14].

To further investigate the hypothesis that EBs maintained greater stemness in μg , we conducted RT-qPCR analysis on stem cell markers, p53 pathway-related genes for cell survival, apoptosis and health, cell cycle regulation, and lineage and tissue type-specific markers.

Significant alterations were found in the Notch and Wnt signaling pathways, which play important roles during embryonic development, including cell fate regulation, cell proliferation, cell differentiation, and cell–cell communication [30–32]. Previous studies have also found alterations in Notch signaling in response to SMG. Specifically, SMG increases differentiation of liver stem cells into hepatocytes through activation of Bmp4/Notch1 signaling [12]. In sharp contrast, our μg experiments show significant downregulation in several Notch signaling genes important for the regulation of cell proliferation and developmental processes (Dvl1, Numb), while neural stem cell development genes were upregulated (DLL3). Interestingly, gene expression markers for neural stem cells and neural development, and terminal differentiation markers for mature neurons (SLC17A6, GALC, and MTAP2) were the only lineage-specific markers that were upregulated in μg compared to 1xg controls (Fig. 6). Previous research also showed increases in nervous system development genes in mesenchymal stem cells flown in space

for 9 days, including genes involved in neuron morphogenesis and transmission of nerve impulses and synapses [33]. However, other studies have shown the negative impact of mechanical unloading on neurogenesis in embryos [34], which may be attributed to impairment of neural migration rather than neural cell development [33]. These results show that neural cells may be one of few whose differentiation from stem cells is not inhibited in the μg environment.

Wnt signaling is known to be altered in μg conditions, although this pathway has mostly been studied in the context of bone formation [35]. In EBs differentiated in μg , the majority of Wnt pathway-related molecules were downregulated, indicating an overall downregulation of the signaling pathway due to unloading. As the Wnt signaling pathways are primarily involved in cell fate determination during embryogenesis and cell proliferation, our results suggest it may also modulate those functions in response to tissue load levels. WNT1 expression, however, increased in μg samples compared with 1xg. WNT1 can induce integrin-dependent differentiation of the neuro-ectoderm lineage, [36] and is also a positive regulator of cardiomyogenesis in mice, which when overexpressed leads to increased cardiomyocyte production and decreased hematopoiesis [37–40]. Increased WNT1 expression is consistent with the observed increased neural marker expression and increased numbers of contractile cardiomyocyte colonies in μg samples.

We also investigated stem cell lineage markers including those for embryonic, hematopoietic, mesenchymal, and neural stem cells in addition to stem cell-specific markers for processes such as metabolism, adhesion, communication, and self-renewal (Figs. 4 and 6). Expression of growth factors associated with stem cell differentiation were significantly decreased in EBs differentiated in μg compared with 1xg, while expression of self-renewal and pluripotency markers (such as SOX1 and SOX2) was less downregulated in μg samples compared with 1xg, indicating partial maintenance of “stemness”.

In contrast, previous studies using SMG have shown decreased “stemness” and increased differentiation in ESCs [41], which may further highlight the discrepancy between modeled μg /SMG and true μg experienced during spaceflight. Since early differentiation of ESCs is associated with signaling via the MAPK pathway, and since this pathway is also associated with mitogenic matrix-integrin-kinase mechanotransduction, it is possible that increased fluid flow in rotating vessels/SMG models may activate signaling that could cause the reported increases in differentiation of stem cells.

One highly downregulated stem cell-specific marker found in μg samples was GJB1, a membrane-spanning protein that forms gap junction channels responsible for signal transduction between neighboring cells through diffusion of molecules such as ions (K^+ and Ca^{2+}), second messengers (IP3 and cAMP), and small metabolites (glucose). Mechanical stimulation causes synthesis of the second messenger molecule, IP3, Ca^{2+} release from intracellular stores, and passage of the Ca^{2+} through gap junctions [42]. Calcium signaling can modulate a number of cell functions such as transcription, proliferation, differentiation, and apoptosis [43,44]. Suppression of GJB1 may disrupt ion channel-based cell communication associated with differentiation.

Among hematopoietic stem cell differentiation markers investigated, increased expression of WNT1 that may cause

suppression of hematopoietic progenitor cell differentiation was found. In addition, terminal differentiation markers for monocytes (CCR5) and macrophages (EMR1) were also significantly downregulated, possibly contributing to the suppression of hematopoietic stem cell differentiation observed in microgravity [14,45–48]. Mesenchymal early stem cell markers including COL1A1, PPAR γ , COL9A1, and ACAN, in addition to late differentiation markers for mesenchymal stem cell lineages were also found to be downregulated in EBs differentiated in μ g, including bone, muscle, and cartilage markers. While adult bone tissue readily degenerates in μ g [49], in EBs we also find downregulation of terminal bone differentiation markers (including CTSK, CALCR, and BGLAP) suggesting early embryonic effects of unloading on bone tissue.

Cartilage-specific differentiation markers, COMP and COL10A1, were also altered in EBs differentiated in μ g (Fig. 6). Cartilage formation is known to be inhibited in microgravity [50]; however, the question remains as to whether decreased cellular activity in cartilage is due to decreased activities of mature cells or an inhibition of differentiation [51]. Muscle is another tissue that is affected by spaceflight-associated μ g mechanical unloading, which results in increased muscle degeneration in response to unloading-induced disuse [52–55]. The downregulation of CAV3, TAGLN, and SMTN in μ g-differentiated EBs compared with 1xg-differentiated EBs may indicate a decreased ability of stem cells to differentiate into smooth muscle.

Decreased gene expression for terminal lineage markers associated with the cardiovascular system, kidneys, and lymphatic system were also noted in μ g EBs (Fig. 6). Specifically, we found decreases in the expression of venous, arterial, and lymphatic endothelium genes including NR2F2, NRP2, NRP1, DLL4, EFNB2, and LYVE1. Vascular endothelial cells are required for functions such as fluid filtration, hemostasis and hormone trafficking, and regulation of the muscle tone in the lumen of blood vessels [56]. Decreased expression of AQP1 and CYP27B1, important molecules for kidney development [57], was also observed in μ g, indicating possible alterations to renal development and function during spaceflight.

Finally, alterations in the differentiation of tissues from the ectoderm and endoderm germ layers were also observed in μ g. Specifically, epidermal lineage markers including KRT1, KRT14, and KRT15, were downregulated while expression of PMEL, a protein expressed in pigment cells, was upregulated in μ g compared with 1xg controls. As keratins are generally found in late stages of epidermal differentiation, it is possible that increased PMEL expression in μ g samples indicated that initiation of epidermal development occurs in μ g but terminal differentiation processes are inhibited [58]. Most terminal differentiation markers for the liver, lung, and pancreas that were investigated in this study also failed to be expressed, or exhibited decreased expression in μ g compared with 1xg controls.

Conclusions

The experiments outlined here aimed to investigate the effects of μ g during spaceflight on the ability of mESCs to differentiate and generate the cell lineages present in terminally differentiated tissues as a model for adult stem cell-based tissue regeneration. To address this question, we ana-

lyzed the influence of μ g on early lineage commitment of stem cells by investigating the ability of EBs to differentiate and develop during the 15 day STL spaceflight experiment in μ g. We found that exposure to μ g inhibits the ability of EBs to differentiate and express terminal differentiation markers for most lineages of the three primary germ layers, including bone, muscle, immune system, renal system, liver, lung, and pancreas (Fig. 6). Furthermore, EBs differentiated in μ g maintained expression of self-renewal markers, indicating partial retention of stem cell properties. EBs differentiated in μ g appeared to initiate the differentiation process but failed to express normal terminal differentiation markers expressed in mechanically loaded tissues. This inhibition of differentiation may be mediated both by incomplete commitment of early stem cell progenitors to the path of differentiation, and later by decreased calcium channel-mediated mechanotransduction signaling. This inhibition of differentiation may not only have significant implications for understanding development in the context of mechanical loading, but also for regeneration of adult mammalian tissues from tissue-specific stem cells. These results provide further evidence for the hypothesis that mechanical unloading of cells and tissues in μ g inhibits the proliferation and differentiation of stem cells resulting in decreased stem cell-based tissue regenerative potential in space and under disuse conditions.

Acknowledgments

This work was supported by NASA Space Life and Physical Sciences Grant NNNH08ZTT003N to Eduardo Almeida. Elizabeth Blaber's work was supported by an Australian Postgraduate Award at University of New South Wales and a Space Biology-funded NASA Postdoctoral Program Fellowship at NASA Ames Research Center.

Author Disclosure Statement

The principal investigator (PI) holds a NASA civil servant Research Scientist position that is similar in nature to a university tenured faculty position that does not depend on the opinions expressed by the scientist. In addition, the NASA funding supporting this work was externally competed based on external scientific peer review, and not intramural review and/or funding that might influence the findings. All other authors were either supported by the PI grant funding or by entities other than NASA such as UNSW. As such, no real competing financial interests exist.

References

1. Lackner JR and P DiZio. (2000). Human orientation and movement control in weightless and artificial gravity environments. *Exp Brain Res* 130:2–26.
2. Sonnenfeld G, JS Butel and WT Shearer. (2003). Effects of the space flight environment on the immune system. *Rev Environ Health* 18:1–17.
3. Davis TA, W Wiesmann, W Kidwell, T Cannon, L Kerns, et al. (1996). Effect of spaceflight on human stem cell hematopoiesis: suppression of erythropoiesis and myelopoiesis. *J Leukoc Biol* 60:69–76.
4. Rapoport EA, LA Goncharova, SA Morenkova and VA Kazarian. (1977). Effect of long-term space flight on protein biosynthesis in different rat tissues and organs. *Kosm Biol Aviakosm Med* 11:20–24.

5. Bergmann O, RD Bhardwaj, S Bernard, S Zdunek, F Barnabe-Heider, et al. (2009). Evidence for cardiomyocyte renewal in humans. *Science* 324:98–102.
6. Smith JA. (1995). Exercise, training and red blood cell turnover. *Sports Med* 19: 9–31.
7. Geuss LR, DC Wu, D Ramamoorthy, CD Alford and LJ Suggs. (2014). Paramagnetic beads and magnetically mediated strain enhance cardiomyogenesis in mouse embryoid bodies. *PLoS One* 9:e113982.
8. McBeath R, DM Pirone, CM Nelson, K Bhadriraju and CS Chen. (2004). Cell shape, cytoskeletal tension, and RhoA regulate stem cell lineage commitment. *Dev Cell* 6:483–495.
9. Tannaz NA, SM Ali, H Nooshin, A Nasser, M Reza, et al. (2014). Comparing the effect of uniaxial cyclic mechanical stimulation and chemical factors on myogenin and Myh2 expression in mouse embryonic and bone marrow derived mesenchymal stem cells. *Mol Cell Biomech* 11:19–37.
10. Wang Y, L An, Y Jiang and H Hang. (2011). Effects of simulated microgravity on embryonic stem cells. *PLoS One* 6:e29214.
11. Li S, Z Ma, Z Niu, H Qian, D Xuan, et al. (2009). NASA-approved rotary bioreactor enhances proliferation and osteogenesis of human periodontal ligament stem cells. *Stem Cells Dev* 18:1273–1282.
12. Majumder S, JH Siamwala, S Srinivasan, S Sinha, SR Sridhara, et al. (2011). Simulated microgravity promoted differentiation of bipotential murine oval liver stem cells by modulating BMP4/Notch1 signaling. *J Cell Biochem* 112:1898–1908.
13. Blaber EA, N Dvorochkin, C Lee, JS Alwood, R Yousuf, et al. (2013). Microgravity induces pelvic bone loss through osteoclastic activity, osteocytic osteolysis, and osteoblastic cell cycle inhibition by CDKN1a/p21. *PLoS One* 8:e61372.
14. Blaber EA, N Dvorochkin, ML Torres, R Yousuf, BP Burns, et al. (2014). Mechanical unloading of bone in microgravity reduces mesenchymal and hematopoietic stem cell-mediated tissue regeneration. *Stem Cell Res* 13:181–201.
15. Dang SM, M Kyba, R Perlingeiro, GQ Daley and PW Zandstra. (2002). Efficiency of embryoid body formation and hematopoietic development from embryonic stem cells in different culture systems. *Biotechnol Bioeng* 78:442–453.
16. Keller GM. (1995). In vitro differentiation of embryonic stem cells. *Curr Opin Cell Biol* 7:862–869.
17. Bain G, D Kitchens, M Yao, JE Huettner and DI Gottlieb. (1995). Embryonic stem cells express neuronal properties in vitro. *Dev Biol* 168:342–357.
18. Palacios R, E Golunski and J Samaridis. (1995). In vitro generation of hematopoietic stem cells from an embryonic stem cell line. *Proc Natl Acad Sci U S A* 92:7530–7534.
19. Rohwedel J, V Maltsev, E Bober, HH Arnold, J Hescheler, et al. (1994). Muscle cell differentiation of embryonic stem cells reflects myogenesis in vivo: developmentally regulated expression of myogenic determination genes and functional expression of ionic currents. *Dev Biol* 164:87–101.
20. Ramalho-Santos M, S Yoon, Y Matsuzaki, RC Mulligan and DA Melton. (2002). “Stemness”: transcriptional profiling of embryonic and adult stem cells. *Science* 298:597–600.
21. Itskovitz-Eldor J, M Schuldiner, D Karsenti, A Eden, O Yanuka, et al. (2000). Differentiation of human embryonic stem cells into embryoid bodies compromising the three embryonic germ layers. *Mol Med* 6:88–95.
22. Bedelbaeva K, A Snyder, D Gourevitch, L Clark, XM Zhang, et al. (2010). Lack of p21 expression links cell cycle control and appendage regeneration in mice. *Proc Natl Acad Sci U S A* 107:5845–5850.
23. Chang SF, TK Chang, HH Peng, YT Yeh, DY Lee, et al. (2009). BMP-4 induction of arrest and differentiation of osteoblast-like cells via p21 CIP1 and p27 KIP1 regulation. *Mol Endocrinol* 23:1827–1838.
24. Esposito F, L Russo, G Chirico, R Ammendola, T Russo, et al. (2001). Regulation of p21waf1/cip1 expression by intracellular redox conditions. *IUBMB Life* 52:67–70.
25. Nargi JL, RR Ratan and DE Griffin. (1999). p53-independent inhibition of proliferation and p21(WAF1/Cip1)-modulated induction of cell death by the antioxidants N-acetylcysteine and vitamin E. *Neoplasia* 1:544–556.
26. Torres M, M Al-Buhairi and G Alsbeih. (2004). Induction of p53 and p21 proteins by gamma radiation in skin fibroblasts derived from breast cancer patients. *Int J Radiat Oncol Biol Phys* 58:479–484.
27. Xie S, Q Wang, L Luo, Q Ruan, T Liu, et al. (2002). Proteasome-dependent downregulation of p21(Waf1/Cip1) induced by reactive oxygen species. *J Interferon Cytokine Res* 22:957–963.
28. Kook SH, YM Jeon, SS Lim, MJ Jang, ES Cho, et al. (2013). Fibroblast growth factor-4 enhances proliferation of mouse embryonic stem cells via activation of c-Jun signaling. *PLoS One* 8:e71641.
29. Kurosawa H, T Imamura, M Koike, K Sasaki and Y Amano. (2003). A simple method for forming embryoid body from mouse embryonic stem cells. *J Biosci Bioeng* 96:409–411.
30. Bigas A, J Guiu and L Gama-Norton. (2013). Notch and Wnt signaling in the emergence of hematopoietic stem cells. *Blood Cells Mol Dis* 51:264–270.
31. Kopan R and MX Ilagan. (2009). The canonical Notch signaling pathway: unfolding the activation mechanism. *Cell* 137:216–233.
32. Hitoshi S, T Alexson, V Tropepe, D Donoviel, AJ Elia, et al. (2002). Notch pathway molecules are essential for the maintenance, but not the generation, of mammalian neural stem cells. *Genes Dev* 16:846–858.
33. Monticone M, Y Liu, N Pujic and R Cancedda. (2010). Activation of nervous system development genes in bone marrow derived mesenchymal stem cells following space-flight exposure. *J Cell Biochem* 111:442–452.
34. Crawford-Young SJ. (2006). Effects of microgravity on cell cytoskeleton and embryogenesis. *Int J Dev Biol* 50: 183–191.
35. Lin C, X Jiang, Z Dai, X Guo, T Weng, et al. (2009). Sclerostin mediates bone response to mechanical unloading through antagonizing Wnt/beta-catenin signaling. *J Bone Miner Res* 24:1651–1661.
36. Czyz J and A Wobus. (2001). Embryonic stem cell differentiation: the role of extracellular factors. *Differentiation* 68:167–174.
37. Weisel KC, HG Kopp, MA Moore, L Studer and T Barberi. (2010). Wnt1 overexpression leads to enforced cardiomyogenesis and inhibition of hematopoiesis in murine embryonic stem cells. *Stem Cells Dev* 19:745–751.
38. Nakamura T, M Sano, Z Songyang and MD Schneider. (2003). A Wnt- and beta-catenin-dependent pathway for mammalian cardiac myogenesis. *Proc Natl Acad Sci U S A* 100:5834–5839.
39. Naito AT, H Akazawa, H Takano, T Minamino, T Nagai, et al. (2005). Phosphatidylinositol 3-kinase-Akt pathway plays a critical role in early cardiomyogenesis by regulating canonical Wnt signaling. *Circ Res* 97:144–151.

40. Kwon C, J Arnold, EC Hsiao, MM Taketo, BR Conklin, et al. (2007). Canonical Wnt signaling is a positive regulator of mammalian cardiac progenitors. *Proc Natl Acad Sci U S A* 104:10894–10899.
41. Wang Y, Y Zhang, S Zhang, G Peng, T Liu, et al. (2012). Rotating microgravity-bioreactor cultivation enhances the hepatic differentiation of mouse embryonic stem cells on biodegradable polymer scaffolds. *Tissue Eng Part A* 18:2376–2385.
42. Boitano S, ER Dirksen and MJ Sanderson. (1992). Intercellular propagation of calcium waves mediated by inositol trisphosphate. *Science* 258:292–295.
43. Berridge MJ. (1993). Inositol trisphosphate and calcium signalling. *Nature* 361:315–325.
44. Berridge MJ, P Lipp and MD Bootman. (2000). The versatility and universality of calcium signalling. *Nat Rev Mol Cell Biol* 1:11–21.
45. Baqai FP, DS Gridley, JM Slater, X Luo-Owen, LS Stodieck, et al. (2009). Effects of spaceflight on innate immune function and antioxidant gene expression. *J Appl Physiol* 106:1935–1942.
46. Sonnenfeld G. (2002). The immune system in space and microgravity. *Med Sci Sports Exerc* 34:2021–2027.
47. Taylor GR, I Konstantinova, G Sonnenfeld and R Jennings. (1997). Changes in the immune system during and after spaceflight. *Adv Space Biol Med* 6:1–32.
48. Zayzafoon M, VE Meyers and JM Mc Donald. (2005). Microgravity: the immune response and bone. *Immunol Rev* 208:267–280.
49. Bikle DD, T Sakata and BP Halloran. (2003). The impact of skeletal unloading on bone formation. *Gravit Space Biol Bull* 16:45–54.
50. Freed LE, R Langer, I Martin, NR Pellis and G Vunjak-Novakovic. (1997). Tissue engineering of cartilage in space. *Proc Natl Acad Sci U S A* 94:13885–13890.
51. Doty SB, D Stiner and WG Telford. (1999). The effect of spaceflight on cartilage cell cycle and differentiation. *J Gravit Physiol* 6:P89–P90.
52. Fitts RH, SW Trappe, DL Costill, PM Gallagher, AC Creer, et al. (2010). Prolonged space flight-induced alterations in the structure and function of human skeletal muscle fibres. *J Physiol* 588:3567–3592.
53. Trappe S, D Costill, P Gallagher, A Creer, JR Peters, et al. (2009). Exercise in space: human skeletal muscle after 6 months aboard the International Space Station. *J Appl Physiol* 106:1159–1168.
54. Vandenberg H, J Chromiak, J Shansky, M Del Tatto and J MLemaire. (1999). Space travel directly induces skeletal muscle atrophy. *FASEB J* 13:1031–1038.
55. Allen DL, ER Bandstra, BC Harrison, S Thorng, LS Stodieck, et al. (2009). Effects of spaceflight on murine skeletal muscle gene expression. *J Appl Physiol* 106:582–595.
56. Vane JR, EE Anggard and RM Botting. (1990). Regulatory functions of the vascular endothelium. *N Engl J Med* 323:27–36.
57. Yoshida N, T Yoshida, A Nakamura, T Monkawa, M Hayashi, et al. (1999). Calcitonin induces 25-hydroxyvitamin D3 1alpha-hydroxylase mRNA expression via protein kinase C pathway in LLC-PK1 cells. *J Am Soc Nephrol* 10:2474–2479.
58. Hellstrom AR, B Watt, SS Fard, D Tenza, P Mannstrom, et al. (2011). Inactivation of Pmel alters melanosome shape but has only a subtle effect on visible pigmentation. *PLoS Genet* 7:e1002285.

Address correspondence to:
Dr. Eduardo A.C. Almeida
Space Biosciences Division
NASA Ames Research Center
Mail Stop 236-7
Moffett Field, CA 94035

E-mail: e.almeida@nasa.gov

Received for publication June 25, 2015

Accepted after revision August 28, 2015

Prepublished on Liebert Instant Online September 28, 2015